Since January 2020 Elsevier has created a COVID-19 resource centre with free information in English and Mandarin on the novel coronavirus COVID-19. The COVID-19 resource centre is hosted on Elsevier Connect, the company's public news and information website.

Available online at www.sciencedirect.com
ScienceDirect
Journal of Molecular Structure 888 (2008) 2–6
Journal of MOLECULAR STRUCTURE
www.elsevier.com/locate/molstruc

Surface-enhanced Raman scattering and DFT computational studies of a benzotriazole derivative

Man-Yu Li [a,b], Qing Liao [a,b], Meng Zhang [c], Xi-Cheng Ai [b,*], Fu-You Li [c,*]

[a] *Beijing National Laboratory for Molecular Science (BNLMS), State Key Laboratory for Structural Chemistry of Unstable and Stable Species, Institute of Chemistry, Chinese Academy of Sciences, Beijing 100080, PR China*
[b] *Department of Chemistry, Renmin University of China, No. 59, ZhongGuanCun Street, Beijing 100872, PR China*
[c] *Department of Chemistry and Laboratory of Advanced Materials, Fudan University, Shanghai 200433, PR China*

Received 17 July 2007; received in revised form 18 October 2007; accepted 12 November 2007
Available online 22 November 2007

Abstract

Here, we report the surface-enhanced Raman scattering (SERS) spectrum of 2-(2′-hydroxy-5′-methylphenyl)benzotriazole (Tinuvin P), a benzotriazole derivative that is the most widely used commercially available UV absorber or stabilizer and is used representatively for the research of photostability mechanism. A full assignment of the Raman spectrum has been made based on the scaled-DFT analysis of the normal vibrational modes. Through the comparative studies on the ordinary Raman spectrum and the SERS spectrum of Tinuvin P, we propose that this molecule binds the Au atom, via the O atom of the hydroxyl or the N1 atom of the benzotriazole moiety, with a perpendicular geometry.

Keywords: Benzotriazole derivative; Surface-enhanced Raman scattering (SERS); Density functional theory (DFT); Adsorption geometry; Adsorptive site

1. Introduction

Benzotriazole derivatives have received increasing interests in chemical, biological and industrial applications. With the high reactivity of the nitrogen sites, they are widely adopted as an important starting material for synthesis [1–3], as the excellent precipitant for metals [4–6], as highly effective corrosion inhibitors which can protect metals from corrosion [7], and most recently, as inhibitor of viral NTPase/helicases such as Hepatitis C virus [8], inhibitor of protein kinase [9–12], Respiratory Syncytial Virus inhibitor [13], inactivator of Severe acute respiratory syndrome (SARS) protease [14] and cytochrome P450 [15], SERRS active label of PNA and DNA [16,17] and radiolabel of tumor [18].

2-(2′-Hydroxy-5′-methylphenyl)benzotriazole (Tinuvin P) features a strong absorption of ultraviolet radiation in the 300–400 nm region with a high degree of photostability over long periods of light exposure, which make Tinuvin P a most widely used commercially available ultraviolet (UV) photostabilizer for a wide variety of polymers against the effects of ultraviolet light. The advantage mentioned above is based on its excited state intramolecular proton transfer (ESIPT) [19].

Knowledge on the molecular geometries and on the active molecular sites in the corresponding molecular complexes is important. Particularly, surface-enhanced Raman scattering (SERS) is known to be sensitive to the local intermolecular charge transfer interaction between the active site of the adsorbate and the effective metal surface [20–22], a piece of information that is crucial for further exploring the chemical and biological applications.

Recently, the density functional theory (DFT) [23,24] combined with the SERS measurement has been successfully applied to investigate the geometry of molecule adsorbed on the effective metal surface, and the full assign-

* Corresponding authors. Tel.: +86 10 62516604; fax: +86 10 62516444.
E-mail address: xcai@chem.ruc.edu.cn (X.-C. Ai).

0022-2860/$ - see front matter © 2007 Elsevier B.V. All rights reserved.
doi:10.1016/j.molstruc.2007.11.019

ment of SERS signals to Raman-active vibrational modes can be achieved [25–27].

We have made use of these well-established spectroscopic and theoretical means to investigate the molecular geometry of Tinuvin P on the surface of gold nanostructure, and to obtain information of intermolecular charge transfer interaction between the active site of Tinuvin P and the gold surface. On the basis of a successful full-assignment of the Raman spectrum, and a comparative study between the ordinary Raman spectrum and the SERS spectrum of Tinuvin P, we conclude that the Tinuvin P molecule binds the Au atom via the O atom of the hydroxyl or the N1 atom of the benzotriazole moiety.

2. Materials and methods

2.1. Materials

Tinuvin P was synthesized according to the reported procedures [28]. The preparation of Au–AAO (anodic aluminum oxide) template-embedded SERS substrate [29] was given in details in Ref. [30]. Briefly, gold was deposited electrochemically into the pores of an AAO template using a silver layer coated on the AAO template as the cathode and a platinum counter electrode as the anode. The silver layer was etched in 8.0 M aqueous HNO_3 for 3–5 min, and then cleaned with distilled water, this procedure was repeated for three times before drying up so as to completely remove the silver layer. Tinuvin P was dissolved in analytical grade dichloromethane (Beijing Chemical Plant, Beijing, China) at a concentration of 1.0×10^{-3} M. The SERS substrate was immersed into the solution for 1–2 min, and then was shaken to remove excess mount of adsorbed sample.

2.2. Raman apparatus

Raman spectra were measured with a liquid-nitrogen cooled CCD detector (SPEC-10-400B/LN, Roper Scientific Research, NJ) attached to a 0.5-m polychromator (grating density 1200 grooves/mm, Spectrapro 550i, Acton Research Corporation, MA). A continuous-wave Ar^+ laser (2060-10S, Spectra Physics, CA) provided the 488 nm Raman excitation beam with a power of 1.5 mW. Raman scattering light was collected in a backscattering geometry and was focused onto the entrance slit of the polychromator after passing through a Raman notch filter (HSNF-488.0-1.5, Kaiser Optical Systems, MI). The Raman spectra were recorded with an exposure time of 15 s and a spectral resolution of 1.4 cm^{-1}. All of the aforementioned sample handling and the Raman measurements were performed at room temperature (298 K).

2.3. Theoretical calculations

The theoretical calculations were performed by using the Gaussian 03W package [31]. The Tinuvin P molecular geometry was optimized by the use of DFT method [23,24] using the hybrid Becke3 (exchange) [32] and the Lee-Yang-Parr (correlation) [33] functional (B3LYP) in conjunction with a modest 6-31G(d) split-valence polarized basis set [34]. The optimization result was shown in Fig. 1. The vibrational frequencies for the optimized structure were calculated by DFT-B3LYP/6-31G(d).

3. Results and discussion

Table 1 lists the observed and the calculated Raman lines. Their full assignments to the Raman active vibration modes are indicated based on the calculated result and the literatures [35,36,27,37]. Since the DFT hybrid B3LYP functional tends to overestimate the frequencies of fundamental modes in comparison to those of the experimentally observed ones, a scaling method is commonly used to obtain a better agreement with the experimental data [38]. Accordingly, for the B3LYP/6-31G(d) method the scale factor of 0.9614 between the observed and calculated wavenumbers was used.

The prediction of Raman intensities was carried out following the procedure outlined below. The calculated Raman activities (S) were converted to relative Raman intensities (I) using the following relation [39],

$$I_i = \frac{f(v_0 - v_i)^4 S_i}{v_i[1 - \exp(-hcv_i/kT)]}, \quad (1)$$

where v_0 and v_i, respectively, are the frequencies (in cm^{-1}) of the exciting wave and the ith normal mode, h, c and k the universal constants, T the temperature, and f is the appropriate scaling factor for all the peak intensities.

3.1. Ordinary Raman spectra

Fig. 2 shows the ordinary Raman spectrum recorded for Tinuvin P in CH_2Cl_2 (10^{-3} M). For comparison, the theoretical Raman spectrum is also shown in Fig. 2, which was constructed with a Gaussian-shape bandwidth of 3 cm^{-1} (FWHM, full width at half maximum). Our result of the ordinary Raman spectrum coincides with that of Kozich's [40], and shows more vibrational Raman lines.

The discrepancy in the observed and the theoretical Raman spectra (Fig. 2) may be due to two reasons: (i) A consequence of the anharmonicity, and the general tendency of overestimation of the force constants at an exact equilibrium geometry in the quantum chemical calculations [41], and (ii) the calculated Raman spectrum represents

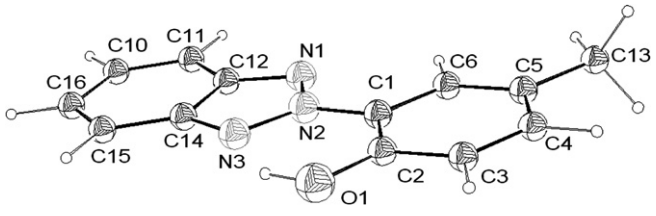

Fig. 1. Optimized geometry of Tinuvin P at the B3LYP/6-31G(d) level.

Table 1
The calculated vibrational frequency (cm^{-1}), ordinary Raman and SERS frequency (cm^{-1}) and their assignments

Calculated	Raman	SERS	Assignment
453	464 (w)	462 (w)	ph_{OH} i.p. deformation
541	545 (w)	544 (w)	bz i.p. deformation
616	625 (w)	623 (w)	bz i.p. deformation
669	678 (w)	676 (w)	ph_{OH} i.p. deformation
883	895 (s)	892 (s)	ph_{OH} i.p. deformation
958	970 (s)	967 (s)	tz i.p. deformation
984	992 (s)	989 (s)	bz i.p. deformation
994	992 (*)	989 (*)	CH3 rocking
1059	1068 (w)	1063 (w)	N–N sy stretch, ph_{OH} i.p. deformation
1115	1131 (w)	1131 (w)	bt C–H i.p. bend
1121	1131 (*)	1131 (*)	ph_{OH} C–H i.p. bend
1223	1215 (vw)	1209 (w)	N–N as stretch + OH i.p. bend
1245	1247 (w)	1242 (w)	N–N as stretch − OH i.p. bend
1269	1267 (vw)	1264 (vw)	C–O stretch
1287	1294 (m)	1291 (s)	ph_{OH} C–H i.p. bend
1306	1300 (m)	1291 (*)	tz ring stretch
1326	1336 (w)	1335 (m)	tz ring stretch, ph_{OH} ring stretch
1338	1345 (w)	1335 (*)	ph_{OH} ring stretch, tz ring stretch
1382	1378 (w)	1383 (w)	O–H i.p. bend, CH_3 sy deformation
1401	1416 (vs)	1413 (vvs)	tz ring stretch, ph_{OH}–N stretch
1435	1444 (vs)	1438 (vs)	bt ring stretch
1456		1464 (w)	CH_3 as deformation
1489	1494 (w)	1489 (w)	bt ring stretch
1505	1512 (m)	1506 (m)	ph_{OH} ring stretch
1553	1562 (m)	1558 (m)	bt ring stretch
1582	1597 (m)	1591 (s)	OH i.p. bend, ph_{OH} ring stretch
1622	1625 (w)	1625 (w)	ph_{OH} ring stretch

Note: i.p., in-plane; o.p., out-of-plane; ph_{OH}, phenol ring; bt, benzotriazole moiety; bz, benzo ring of bt; tz, triazole ring of bt; sy, symmetric; as, antisymmetric; (*), band overlapped.

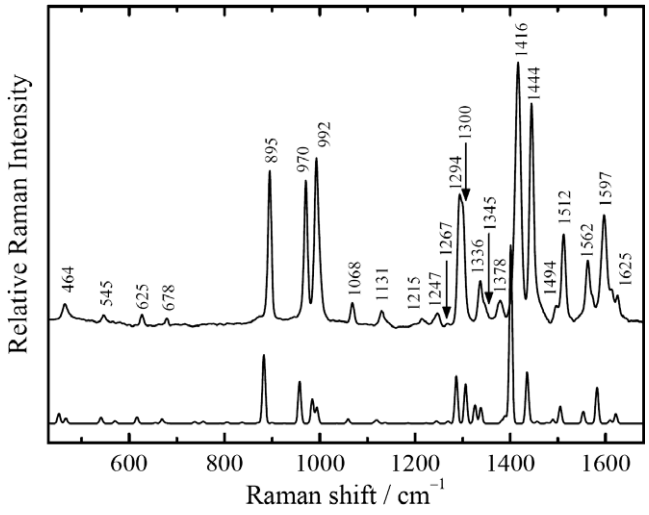

Fig. 2. Ordinary (upper) and theoretical (lower) Raman spectra of Tinuvin P. The ordinary spectrum was measured for Tinuvin P in CH_2Cl_2 (1.0×10^{-3} M) and solvent contributions are subtracted. The theoretical spectrum was constructed with a Gaussian-shape bandwidth of 3 cm^{-1} (full width at half maximum). The excitation laser power was 1.5 mW at 488 nm.

vibrational signatures for molecules in gas phase, whereas the experimental Raman spectrum is in solution.

3.2. SERS spectra

Fig. 3 shows the SERS spectrum (curve-a) and the ordinary Raman spectrum (curve-b) of Tinuvin P adsorbed on to Au-AAO and bare AAO template, respectively. Only six peaks at 892, 970, 987, 1299, 1411 and 1441 cm^{-1} can be recognized clearly in the ordinary spectrum without enhancement. The SERS spectrum with a greatly improved signal-to-noise ratio exhibits clear Raman lines. The absolute intensity of the SERS spectrum was enhanced by a factor of ~40 with reference to the ordinary one on bare AAO template as estimated from the data in Fig. 3.

It is seen from Fig. 4 that compared to the ordinary Raman spectrum in solution, most of the SERS bands become a little broader and frequency-shift. The Raman bands at 1264 and 1464 cm^{-1} shows very strong enhancement (the Cartesian displacements shows in Fig. 5). The intense bands at 1413, 1438, 1506, 1558, 1591 cm^{-1} in the SERS spectrum are similar to the bands of the ordinary Raman spectrum, and the bands show strong enhancement and frequency-shift with respect to the ordinary Raman spectrum of Tinuvin P solution. The bands at 1291 and 1335 cm^{-1} are the overlapping of two ordinary Raman bands, respectively, with little frequency-shift and strong enhancement. As demonstrated in Fig. 4, the relative intensities of SERS bands at 892, 967 and 989 cm^{-1} are similar to those of the ordinary Raman spectrum, and no frequency-shifts upon adsorption were observed. These spectral differences were induced by the interaction between the substrate of template-embedded gold array and the Tinuvin P adsorbate, which may considerably alter the polarizability tensor of the Tinuvin P molecule [42].

According to the surface selection rules [43–47], for adsorbed molecules, the vibrations with the polarizability derivative components perpendicular to the surface will be enhanced more. Based on this consideration, the molec-

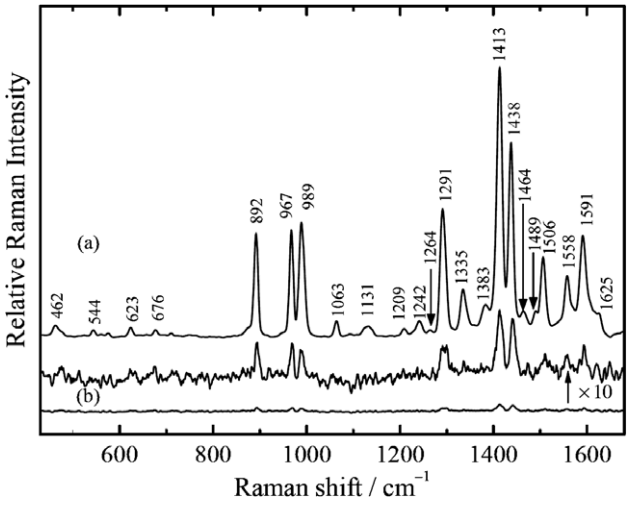

Fig. 3. (a) SERS spectrum of Tinuvin P adsorbed onto Au-AAO substrate. (b) Raman spectrum of Tinuvin P adsorbed onto the bare AAO template. The excitation laser power was 1.5 mW at 488 nm.

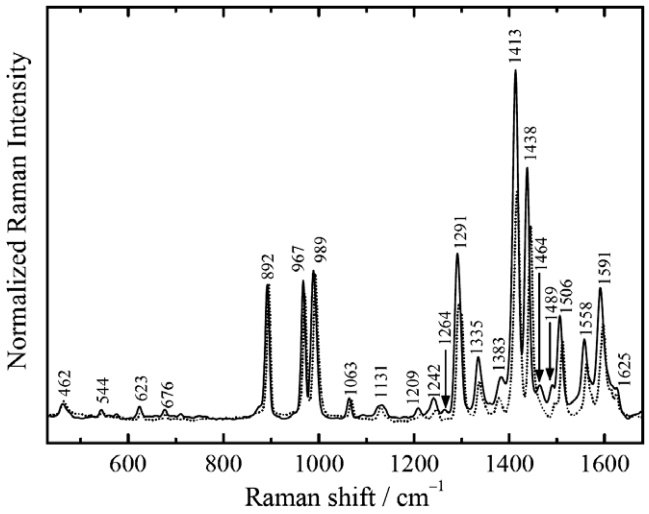

Fig. 4. Comparison between the SERS spectrum (solid) and the ordinary Raman spectrum in CH_2Cl_2 (1.0×10^{-3} M) (dotted) of Tinuvin P. Solvent contributions are subtracted.

ular orientation of the adsorbate on the surface of Au nanorods can be deduced.

It is seen from Fig. 3 that both the ring-stretch and the in-plane-bending modes were strongly enhanced, the polarizability tensor of the modes may perpendicular to the Au surface. According to the optimized Tinuvin P geometry (Fig. 1) which together with the crystallographic data [48], the benzotriazole and the phenol rings in Tinuvin P molecule are coplanar, thus the Tinuvin P molecule must be perpendicular to or tilted on the metal surface. There are no vibrational modes of out-of-plane ring bending appearing in the ordinary or SERS spectrum, therefore, it is concluded that the molecule is perpendicular to the Au surface.

The molecule may bind to the gold surface with a perpendicular geometry through the lone pair electrons of either the nitrogen (N1 and N3) or oxygen (O1) atom or through both of them. Apparently the N3 atom avoids any gold–nitrogen interaction owing to the steric hindrance caused by the O atom. A more favored adsorptive site can be enumerated theoretically by estimating the atomic charges on each of these probable active sites [49]. Higher the negative charge density on the atom, higher the probability of it acting as an adsorptive site for the gold substrate. Theoretical results estimated from calculations show that the partial atomic charges on the nitrogen and oxygen atoms determined by the natural population analysis (NPA) are −0.255 (N1) and −0.692 (O1), respectively. The negative charge density is observed on O1 atom and N1 atom, thereby the active may involve these atoms in the adsorption process. The enhancement decreases rapidly as a function of distance from the Au surface. The bands at 1264 and 1464 cm^{-1} which are ascribed to the C–O stretch and CH_3 asymmetric deformation, respectively, both exhibit very strong enhancement in SERS spectrum, this evidence substantiates involvement of O1 atom and N1 atom in the adsorption process.

On the basis of the above discussion, we propose that the Tinuvin P molecule binds the metal surface via two possible contacting sites, i.e., the O atom of the hydroxyl or the N1 atom of the benzotriazole moiety. In both cases the planar Tinuvin P molecule was perpendicular on the Au surface, which is schematically illustrated in Fig. 6a, b, respectively.

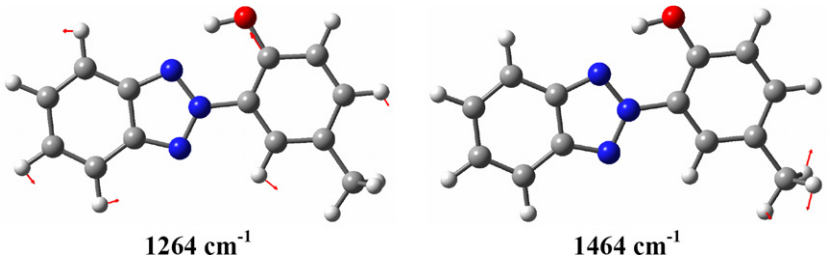

Fig. 5. The Cartesian displacements of some relevant vibrational modes with the Raman-shift in SERS spectrum.

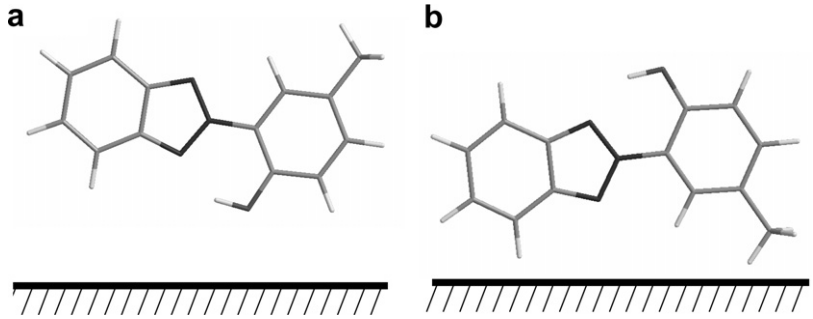

Fig. 6. Schematic illustration of the adsorption geometries of Tinuvin P molecules on the Au surface ((a) via O atom (b) via N1 atom).

4. Conclusions

To summarize, the high quality SERS spectrum of 2-(2′-hydroxy-5′-methylphenyl)benzotriazole (Tinuvin P) adsorbed on the AAO-template-embedded array of Au nanorods is reported in the present work. A full assignment of the Raman spectrum was made based on the scaled-DFT analysis of the normal vibrational modes. On the basis of a comparative study between the ordinary Raman and the SERS spectra of Tinuvin P, we propose that the Tinuvin P molecule, which binds Au atom via the O atom of the hydroxyl or the N1 atom of the benzotriazole moiety, adopt two possible orientations on the Au surface with a perpendicular geometry.

Acknowledgements

This work has been supported by the Natural Science Foundation of China (Grants #20673144 and #20433010).

References

[1] A.R. Katritzky, S.A. Belyakov, Aldrichim. Acta 31 (1998) 35.
[2] A.R. Katritzky, X. Lan, J.Z. Yang, O.V. Denisko, Chem. Rev. 98 (1998) 409.
[3] A. Dondoni, A. Marra, Chem. Rev. 104 (2004) 2557.
[4] J.A. Curtis, Ind. Eng. Chem. Anal. Ed. 13 (1941) 349.
[5] K.L. Cheng, Anal. Chem. 26 (1954) 1038.
[6] R.F. Wilson, L.E. Wilson, Anal. Chem. 28 (1956) 93.
[7] Y.C. Wu, P. Zhang, H.W. Pickering, D.L. Allara, J. Electrochem. Soc. 140 (1993) 2791, and references therein.
[8] P. Borowski, J. Deinert, S. Schalinski, M. Bretner, K. Ginalski, T. Kulikowski, D. Shugar, Eur. J. Biochem. 270 (2003) 1645.
[9] R. Battistutta, E. De Moliner, S. Sarno, G. Zanotti, L.A. Pinna, Protein Sci. 10 (2001) 2200.
[10] S. Mishra, A. Reichert, J. Cunnick, D. Senadheera, B. Hemmeryckx, N. Heisterkamp, J. Groffen, Oncogene 22 (2003) 8255.
[11] G. Scapin, S.B. Patel, J.W. Becker, Q. Wang, C. Desponts, D. Waddleton, K. Skorey, W. Cromlish, C. Bayly, M. Therien, J.Y. Gauthier, C.S. Li, C.K. Lau, C. Ramachandran, B.P. Kennedy, E. Asante-Appiah, Biochemistry 42 (2003) 11451.
[12] O. Abramczyk, P. Zień, R. Zieliński, M. Pilecki, U. Hellman, R. Szyszka, Biochem. Biophys. Res. Commun. 307 (2003) 31.
[13] K.-L. Yu, Y. Zhang, R.L. Civiello, K.F. Kadow, C. Cianci, M. Krystal, N.A. Meanwell, Bioorg. Med. Chem. Lett. 13 (2003) 2141.
[14] C.-Y. Wu, K.-Y. King, C.-J. Kuo, J.-M. Fang, Y.-T. Wu, M.-Y. Ho, C.-L. Liao, J.-J. Shie, P.-H. Liang, C.-H. Wong, Chem. Biol. 13 (2005) 261.
[15] U.M. Kent, J.R. Bend, B.A. Chamberlin, D.A. Gage, P.F. Hollenberg, Chem. Res. Toxicol. 10 (1997) 600.
[16] D. Graham, R. Brown, W.E. Smith, Chem. Comm. 11 (2001) 1002.
[17] R. Brown, W.E. Smith, D. Graham, Tetrahedron Lett. 44 (2003) 1339.
[18] F.G. van Schaijk, M. Broekema, E. Oosterwijk, J.E.M. van Eerd, B.J. McBride, D.M. Goldenberg, F.H.M. Corstens, O.C. Boerman, J. Nucl. Med. 46 (2005) 1016.
[19] T. Fournier, S. Pommeret, J.-C. Mialocq, A. Deflandre, R. Rozot, Chem. Phys. Lett. 325 (2000) 171, and references therein.
[20] M. Moskovits, Rev. Mod. Phys. 57 (1985) 783.
[21] A. Otto, J. Raman Spectrosc. 36 (2005) 497.
[22] Q. Zhou, X.W. Li, Q. Fan, X.X. Zhang, J.W. Zheng, Angew. Chem. Int. Ed. 45 (2006) 3970.
[23] P. Hohenberg, W. Kohn, Phys. Rev. 136 (1964) B864.
[24] W. Kohn, L.J. Sham, Phys. Rev. 140 (1965) A1133.
[25] T. Iliescu, D. Maniu, V. Chis, F.D. Irimie, Cs. Paizs, M. Tosa, Chem. Phys. 310 (2005) 189.
[26] M. Baia, L. Baia, W. Kiefer, J. Popp, J. Phys. Chem. B 108 (2004) 17491.
[27] J. Sarkar, J. Chowdhury, M. Ghosh, R. De, G.B. Talapatra, J. Phys. Chem. B 109 (2005) 12861.
[28] Z.M. Ding, Z.Y. Guo, Plast. Addit. 6 (2004) 15.
[29] S.J. Lee, A.R. Morrill, M. Moskovits, J. Am. Chem. Soc. 128 (2006) 2200.
[30] C. Mu, Y.X. Yu, R.M. Wang, K. Wu, D.S. Xu, G.L. Guo, Adv. Mater. 16 (2004) 1550.
[31] M.J. Frisch, G.W. Trucks, H.B. Schlegel, G.E. Scuseria, M.A. Robb, J.R. Cheeseman, J.A. Montgomery Jr., T. Vreven, K.N. Kudin, J.C. Burant, J.M. Millam, S.S. Iyengar, J. Tomasi, V. Barone, B. Mennucci, M. Cossi, G. Scalmani, N. Rega, G.A. Petersson, H. Nakatsuji, M. Hada, M. Ehara, K. Toyota, R. Fukuda, J. Hasegawa, M. Ishida, T. Nakajima, Y. Honda, O. Kitao, H. Nakai, M. Klene, X. Li, J.E. Knox, H.P. Hratchian, J.B. Cross, C. Adamo, J. Jaramillo, R. Gomperts, R.E. Stratmann, O. Yazyev, A.J. Austin, R. Cammi, C. Pomelli, J.W. Ochterski, P.Y. Ayala, K. Morokuma, G.A. Voth, P. Salvador, J.J. Dannenberg, V.G. Zakrzewski, S. Dapprich, A.D. Daniels, M.C. Strain, O. Farkas, D.K. Malick, A.D. Rabuck, K. Raghavachari, J.B. Foresman, J.V. Ortiz, Q. Cui, A.G. Baboul, S. Clifford, J. Cioslowski, B.B. Stefanov, G. Liu, A. Liashenko, P. Piskorz, I. Komaromi, R.L. Martin, D.J. Fox, T. Keith, M.A. Al-Laham, C.Y. Peng, A. Nanayakkara, M. Challacombe, P.M.W. Gill, B. Johnson, W. Chen, M.W. Wong, C. Gonzalez, J.A. Pople, Gaussian 03W, Revision B.01, Gaussian, Inc., Pittsburgh, PA, 2003.
[32] A.D. Becke, J. Chem. Phys. 98 (1993) 5648.
[33] C. Lee, W. Yang, R.G. Parr, Phys. Rev. B 37 (1988) 785.
[34] R. Ditchfield, W.J. Hehre, J.A. Pople, J. Chem. Phys. 54 (1971) 724.
[35] A.A. Jbarah, A. Ihle, K. Banert, R. Holze, J. Raman Spectrosc. 37 (2006) 123.
[36] A.A. Jbarah, K. Banert, R. Holze, Vib. Spectrosc. 44 (2007) 142.
[37] J. Sarkar, J. Chowdhury, G.B. Talapatra, J. Phys. Chem. C 111 (2007) 10049.
[38] A.P. Scott, L. Radom, J. Phys. Chem. 100 (1996) 16502.
[39] P.L. Polavarapu, J. Phys. Chem. 94 (1990) 8106.
[40] V. Kozich, J. Dreyer, S. Ashihara, W. Werncke, T. Elsaesser, J. Chem. Phys. 125 (2006) 074504.
[41] G. Rauhut, P. Pulay, J. Phys. Chem. 99 (1995) 3093.
[42] T. Iliescu, F.D. Irimie, M. Bolboaca, Cs. Paisz, W. Kiefer, Vib. Spectrosc. 29 (2002) 251.
[43] M. Moskovits, J.S. Suh, J. Phys. Chem. 88 (1984) 5526.
[44] J.S. Suh, M. Moskovits, J. Am. Chem. Soc. 108 (1986) 4711.
[45] M. Moskovits, D.P. DiLella, K.J. Maynard, Langmuir 4 (1988) 67.
[46] M. Moskovits, J.S. Suh, J. Phys. Chem. 92 (1988) 6327.
[47] X.P. Gao, J.P. Davies, M.J. Weaver, J. Phys. Chem. 94 (1990) 6858.
[48] J. Catalán, J.L.G. de Paz, M.R. Torres, J.D. Tornero, J. Chem. Soc. Faraday Trans. 93 (1997) 1691.
[49] J. Chowdhury, M. Ghosh, T.N. Misra, Spectrochim. Acta A 56 (2000) 2107.